Hindawi
Advances in Civil Engineering
Volume 2022, Article ID 6931212, 20 pages
https://doi.org/10.1155/2022/6931212

Research Article

Performance of Structure Equipped AP-TMD Compared with MTMD, ATMD, and PTMD against Earthquake Using Genetic Fuzzy Algorithm

F. Hadizadeh, F. Akhlaghi Amiri, and H. Shariatmadar

Department of Civil Engineering, Ferdowsi University of Mashhad, Mashhad, Iran

Correspondence should be addressed to H. Shariatmadar; shariatmadar@um.ac.ir

Received 27 May 2022; Revised 10 July 2022; Accepted 21 July 2022; Published 29 August 2022

Academic Editor: Loke Kok Foong

During the past years, different control devices have been introduced and used to reduce the response of structures. This article presents the performance of active-passive tuned mass dampers (AP-TMDs) in the reduction of structural responses and a comparison between the uses of different controllers, including tuned mass damper (TMD), active tuned mass damper (ATMD), and multituned mass damper (MTMD). Analyzing and modeling the structure under four near- and far-field earthquakes are performed in MATLAB and SIMULINK. Finally, the responses of controlled and uncontrolled structures equipped with these controllers are investigated. Fuzzy and genetic-based fuzzy logic controllers are used to determine the control force of ATMD and AP-TMD, respectively. In order to compare the performance of the dampers, the mass ratio of TMDs is fixed in all cases and is taken to be 5%. Damping of the structure is considered equal to 5%. The frequency and damping ratio of TMDs with maximum and RMS displacement optimization criteria are obtained. The mass ratio of TMDs in controlled structures with MTMD and AP-TMD is calculated by numerical analysis. It can be inferred that using control force affects response reduction in both ATMD and AP-TMD controllers significantly. In addition, using AP-TMD can bring the merits of both passive and active systems by providing active control and reducing power requirements for control forces. All controllers are recommended for structural control although AP-TMD reduced maximum and RMS displacement by about 50% in the best case, which has better performance than others. On the other hand, ATMD decreased RMS acceleration by 37.5% on average in four earthquakes compared to the uncontrolled structure.

1. Introduction

Nowadays, structural control is advanced significantly, and in turn, many control devices and algorithms have been proposed [1–3] since vibration leads to structural damage in extreme loads [4].

It is commonly stated by researchers and engineers that passive systems are the simplest structural response control systems that require no power [5]. A tuned mass damper (TMD), as a control device, can decrease the response of high-rise buildings arising from earthquakes and wind, but the detuning effect of TMD results in exhausting the seismic resistance of TMD, which should be addressed for more effectiveness. A TMD is usually installed on the higher floors of a building due to occurring maximum displacement there to absorb the external forces [6]. Selecting proper parameters in TMD can greatly improve the damping performance [7]. TMD is used in actual applications, and shaking table tests are used in many research. In research, to investigate the vibration control effects of a tuned mass damper on the monopile offshore wind turbine tower under wind-wave and seismic excitations, shaking table tests are used [8]. In another article, the vibration control effects of a five-story steel frame equipped with PTMD under seismic excitation are investigated by a series of shaking table tests [9]. The performance of a one-story steel frame attached with a particle tuned mass damper is investigated through free vibration and shaking table test [10]. TMD has different drawbacks; for example, TMD may leak over time, thus limiting the service life. The physical properties may degrade in high-

temperature environments, resulting in failure [11]. The stiffness of the overall system increases because of the viscous dampers, which is unexpected for some structures. To overcome some deficiencies of traditional tuned mass damper, Eddy-current tuned mass dampers (EC-TMDs) are suggested as noncontacting passive control devices that induce a magnetic field with opposite polarity, causing repulsive forces, i.e., damping forces [12].

When a structure shows a nonlinear behavior under strong wind or earthquake, the reduction of the basic natural frequency of the structure changes the frequency ratio of the TMD, and in turn, TMD cannot absorb the energy of earthquakes or wind, which is named the "detuning effect" of a TMD [6]. Totally, the traditional TMD, which has a fixed frequency, cannot perform effectively against earthquakes due to the frequency variations [13].

To mitigate or obviate this demerit, researchers have proposed many approaches [1, 6, 14–25]. For example, the advent of multiple tuned mass dampers (MTMDs) [26] has modified this deficiency. In addition, another limitation of a TMD is the size of its mass. Therefore, it is attempted to solve this limitation and increase the performance of the TMD. In this regard, different control devices have been represented [27–30].

An ATMD, as a controller employed in structure, consists of a tuned mass damper (TMD) and an actuator [31]. Active control systems require a large power source for the operation to provide the control forces for the actuator. Although many researchers have proved the efficiency of using ATMD [32, 33], it has two main weak points. First, applying the active control requires high-capacity equipment generating control force. Second, sophisticated sensing and signal-processing systems are required for the operation of active systems [5].

One way of increasing TMD's effectiveness and decreasing TMD's limitations is using hybrid mass dampers consisting of a combination of an AMD and a TMD introduced by Cheng [34]. In this system, the AMD is attached to the TMD instead of to the structure; therefore, the mass of AMD can be between 10% and 15% of that of the TMD. The control force used in the system regulates the TMD and thus increases the device's efficiency and robustness to change the structure's dynamic characteristics. In other words, the TMD is tuned to the fundamental mode of the structure, and the AMD is designed to improve control effectiveness for higher modes of the structure. Thus, such a system has two main merits. First, the energy and forces required to operate an HMD are far less than an AMD system with similar performance. Second, the space limitation for using TMD results in the privilege of AMD. Due to these reasons, HMDs are relatively inexpensive and the most common control device used in buildings [35–37].

Some scientists presented an active-passive composite mass damper system for controlling vibration of base excitation, which illustrates the significant reduction in peak structural response compared with a single passive mass damper system [38].

In another research, Nishimura et al. [39] proposed ATMD attached to TMD, which is named active-passive tuned mass damper (AP-TMD)]. They reached out that AP-TMD has many benefits, including a smaller size of the active controller than that of ATMD and a smaller required control force or power for activating the controller than that of the expected vibration control performance. In this regard, much research has been done in recent years [38, 40, 41]. This system has already been installed in previous years in the 145-meter Dowa Phoenix Tower in Osaka, Japan [38].

Moreover, another system consisting of multi-active-passive tuned mass dampers (APTMDs) with a uniform distribution of natural frequencies has been proposed by Chunxiang, and it is named multiple active-passive tuned mass dampers (MAPTMD). In a MAPTMD system, the stiffness and damping coefficient is considered constant while the mass varies. In this study, the control forces for MAPTMD are generated based on displacement and velocity feedback gain and changing the acceleration feedback gain. Finally, the results of using AP-TMD are compared with MAPTMD and show that using MAPTMD can reduce the oscillations of structures under earthquakes. Also, it is shown that the MAPTMD can obtain high robustness and has better effects than a single AP-TMD. In particular, since using an ATMD requires a large active control force, MAPTMD is more applicable than an AP-TMD [42].

Many different algorithms can be employed to make control force in active controllers. Utilization of fuzzy logic controllers (FLC) for estimating control force are investigated in many types of research [43–49] and have been employed due to lots of advantages.

Fuzzy Logic (FL) was introduced in 1965 by Lotfi Zadeh [50]. Fuzzy logic as an expert system uses linguistic variables in order to make a rule base [51]. Fuzzy controllers cover many different operating conditions. This system, which has different advantages, is widely investigated [52, 53]. In introducing fuzzy logic, it can be said that fuzziness is the opposite of precision. Indeed, everything without a precise definition or clear description of boundaries in space or time is considered a bearer of fuzziness, which is stated by Herbert [51].

Recently, genetic algorithms have shown significant interest due to their ability to solve complex problems. For the first time, Holland [54] introduced and Goldberg [55] implemented these ideas in the simple genetic algorithm (SGA). The main concepts of the simple genetic algorithm (SGA) coming from natural selection in Darwin's theory have four steps: first, evaluate each individual's fitness in the problem environment; second, choose a new population of individuals based on relative fitness; third, exchange information between individuals using crossover; fourth, mutate individuals randomly.

After several generations, the algorithms converge to the best chromosome, which is almost the optimal solution [56].

Recent research showed that the merits of using controllers, whether passive or active, in the reduction of structural response with their negative and positive points but using AP-TMD as a controller with genetic fuzzy algorithms have not been investigated so far; therefore, in this article, the performance of active-passive tuned mass damper in an 11-story building is compared with other controllers either active or passive ones. Moreover, fuzzy and

genetic fuzzy algorithms are employed to generate control forces in active controllers, and all results regarding their performance are presented.

2. Structural Modeling

In this article, a real 11-story building (2D dimension) is used to consider the effects of various controllers in the reduction of structural response. In this structure, the floors are completely rigid, and one degree of transitional freedom is considered for each floor. This shear structure with n degree of freedom, when equipped with a tuned mass damper installed at the roof level, can be considered as a structure $(n+1)$ degree of freedom. When a TMD or MTMD (in which two mass dampers are connected in series) is installed on the roof of the structure, the number of degrees of freedom must be considered $(n+1)$ or $(n+2)$, respectively. The equation of motion of this system under seismic excitation can be seen in the following equation:

$$M.\ddot{U}(t) + C.\dot{U}(t) + K.U(t) = -M.E.\ddot{U}_g, \tag{1}$$

where M is the mass of system, C is its damping, and K is the stiffness. U is the horizontal displacement vector of the floors relative to the ground and E is the effect vector.

If the control force is used in the controller (for ATMD, AP-TMD), the following equation will be written:

$$M.\ddot{U}(t) + C.\dot{U}(t) + K.U(t) = -M.E.\ddot{U}_g + E_f.F, \tag{2}$$

where F is the control force and E_f is the displacement vector of the control force. In this equation, $\ddot{U}$, $\dot{U}$, and U represent the floor acceleration, velocity, and displacement vectors and $\ddot{U}_g$ is the vector of ground acceleration. The matrix of M, C, K, U, E, E_f is shown as follows:

$$M = \operatorname{diag}[m_1, m_2, \ldots, m_n, m_{d1}, m_{d2}], \tag{3}$$

$$U(t) = \begin{Bmatrix} U_1(t) \\ U_2(t) \\ U_3(t) \\ \vdots \\ U_n(t) \\ U_{d1}(t) \\ U_{d2}(t) \end{Bmatrix}, \tag{4}$$

$$K = \begin{bmatrix} (K_1+K_2) & -K_2 & \ldots & \ldots & \ldots & \ldots & 0 \\ -K_2 & (K_2+K_3) & -K_3 & \ldots & \ldots & \ldots & \ldots \\ \vdots & -K_3 & \ldots & \vdots\ddots & -K_n & \ldots & \vdots \\ \ldots & \ldots & \ldots & -K_n & (K_n+K_{d1}) & -K_{d1} & \ldots \\ \ldots & \ldots & \ldots & \ldots & -K_{d1} & (K_{d1}\,|+K_{d2}) & -K_{d2} \\ 0 & \ldots & \ldots & \ldots & \ldots & -K_{d2} & K_{d2} \end{bmatrix}, \tag{5}$$

$$C = \begin{bmatrix} (C_1+C_2) & -C_2 & \ldots & \ldots & \ldots & \ldots & 0 \\ -C_2 & (C_2+C_3) & -C_3 & \ldots & \ldots & \ldots & \ldots \\ \vdots & -C_3 & \ldots & \ddots & -C_n & \ldots & \vdots \\ \ldots & \ldots & \ldots & -C_n & (C_n+C_{d1}) & -C_{d1} & \ldots \\ \ldots & \ldots & \ldots & \ldots & -C_{d1} & (C_{d1}+C_{d2}) & -C_{d2} \\ 0 & \ldots & \ldots & \ldots & \ldots & -C_{d2} & C_{d2} \end{bmatrix}, \tag{6}$$

$$E = \begin{Bmatrix} 1 \\ 1 \\ \vdots \\ 1 \end{Bmatrix}_{(n+2)*1}, \tag{7}$$

$$E_f = \begin{Bmatrix} [0]_{(n*1)} \\ 1 \\ -1 \end{Bmatrix}. \tag{8}$$

In these equations, d1 and d2 are related to two TMD in roof (MTMD).

Equation (1) can be written in the form of state space as follows:

$$\dot{X} = A.X + B_f.F + B_g.\ddot{U}_g, \tag{9}$$

$$X = \left\{ \begin{array}{c} \{U\}_{(n+2)*1} \\ \left\{\dot{U}\right\}_{(n+2)*1} \end{array} \right\}, \tag{10}$$

$$A = \left[\begin{array}{cc} [0]_{(n+2)*(n+2)} & [I]_{(n+2)*(n+2)} \\ \left[-M^{-1}, K\right]_{(n+2)*(n+2)} & \left[-M^{-1}, C\right]_{(n+2)*(n+2)} \end{array} \right], \tag{11}$$

$$B_f = \left\{ \begin{array}{c} \{0\}_{(n+2)*1} \\ \left\{M^{-1}.E_f\right\}_{(n+2)*1} \end{array} \right\}, \tag{12}$$

$$B_g = \left\{ \begin{array}{c} \{0\}_{(n+2)*1} \\ \{-E\}_{(n+2)*1} \end{array} \right\}. \tag{13}$$

I is an identity matrix.

The characteristics related to the mass and stiffness of the floors of this structure can be seen in Table 1 [41]. It should also be noted that the damping of the structure is considered equal to 5%.

The Rayleigh method is used to estimate the structure's damping, which is obtained from the following equations:

$$[C] = a_0[M] + b_0[K], \tag{14}$$

$$a_0 = \zeta_i \left[\frac{2\omega_i.\omega_j}{\omega_i + \omega_j}\right], \tag{15}$$

$$b_0 = \zeta_i \left[\frac{2}{\omega_i + \omega_j}\right]. \tag{16}$$

The parameters used above are elaborated as follows:

a_0 and b_0 are coefficients of proportionality

ω_i and ω_j are modal frequencies of structures related to modes i and j

ζ_i and ζ_j are damping ratios of structures pertaining to modes i and j

In this research, the first and second modes have been used.

3. The Properties of Controllers

In this study, the performance of passive tuned mass damper (PTMD), active tuned mass damper (ATMD), multiple tuned mass damper (MTMD), and active-passive tuned mass damper (AP-TMD) in reducing the response of the structure is investigated. The mass ratio of dampers to the mass of the structure is displayed with (μ). To compare the performance of the dampers, μ is fixed in all cases and is taken to be 5%. To determine the frequency ratio (α) in the range 0.5 to 1.5 to the frequency of the structure and for the damping ratio (ζ) in the range 0 to 0.15, these two parameters (α, ζ) are optimized based on the combination of maximum and RMS displacement of the structural roof. In the combined criterion, optimization is performed based on a combination of a 70% reduction in maximum roof displacement and 30% RMS structural roof displacement. In other words, the values of frequency ratio and damping ratio of TMDs have been optimized to reduce the two mentioned criteria. The optimization results for the control parameters show that the parameters (frequency ratio and damping ratio) for different earthquakes and different control systems are completely variable. Therefore, it is necessary to select the type of control system and the regulating parameters according to the seismic characteristics of the region and its acceleration. Such parameters should be optimized and then the systems are analyzed and evaluated.

Table 1: Mass and stiffness of each floor.

Story	Mass (kg)	Stiffness (N/m)
1	215370	4.68 *e* 8
2	201750	4.76 *e* 8
3	201750	4.68 *e* 8
4	200930	4.50 *e* 8
5	200930	4.50 *e* 8
6	200930	4.50 *e* 8
7	203180	4.50 *e* 8
8	202910	4.37 *e* 8
9	202910	4.37 *e* 8
10	176100	4.37 *e* 8
11	66230	3.12 *e* 8

Equations (17)–(19) have been used to adjust and control the stiffness and damping parameters of dampers.

$$\omega_{\text{tmd}} = \alpha \times \omega_{\text{structure}}, \tag{17}$$

$$K_{\text{tmd}} = \omega_{\text{tmd}}^2 \times m_{\text{tmd}}, \tag{18}$$

$$c_{\text{tmd}} = 2 \times m_{\text{tmd}} \times \omega_{\text{tmd}} \times \zeta_{\text{opttmd}}. \tag{19}$$

3.1. Passive Tuned Mass Damper Controller. This n-story structure with a TMD at the roof level can be considered a structure $(n + 1)$ degree of freedom. Table 2 shows the optimized frequency ratio and damping ratio of PTMD for each earthquake based on the combined combination of maximum and RMS displacement.

3.2. Active Tuned Mass Damper Controller. In this controller, control force is used to improve the performance of the system and reduce the structural response.

Table 3 shows the optimized frequency ratio and damping ratio of ATMD for each earthquake based on the combined combination of maximum and RMS displacement. The control force is calculated by a fuzzy logic algorithm. The fuzzy logic is described in section 6.

Table 2: Damping ratio and frequency ratio of PTMD.

PTMD	Earthquakes	Frequency ratio of the first TMD	Damping ratio of the first TMD
	El Centro	0.78	0.15
	Hachinohe	0.71	0.15
	Kobe	0.9	0.02
	Northridge	0.98	0.15

Table 3: Damping ratio and frequency ratio of ATMD.

ATMD	Earthquakes	Frequency ratio of the first TMD	Damping ratio of the first TMD
	El Centro	1	0.14
	Hachinohe	0.8	0.01
	Kobe	0.87	0.04
	Northridge	0.89	0.04

3.3. Multituned Mass Damper Controller. In this system, two TMDs are connected to each other in series. To select the appropriate mass ratio of the two TMDs, the structure equipped with MTMD with different distributions of mass ratio was investigated:

$$M_{\text{tmd}} = \mu \times M_{\text{Structure}}, \tag{20}$$

$$\mu = \frac{M_{\text{TMD1}} + M_{\text{TMD2}}}{M_{\text{structure}}} = 5\%, \tag{21}$$

$$\frac{M_{\text{TMD1}}}{M_{\text{TMD1}} + M_{\text{TMD2}}} = 80\%. \tag{22}$$

In this relation, $M_{\text{Structure}}$ is the mass of the structure and μ is the mass ratio of TMDs in the structure. Moreover, M_{TMD1} and M_{TMD2} are the mass of first and second TMD, respectively.

Table 4 shows the optimized frequency ratio and damping ratio of MTMD for each earthquake based on the combined combination of maximum and RMS displacement. The calculation of α and ζ for MTMD dampers is done numerically.

For example, Table 5 presents the displacement of the roof of the structure and the displacement of two TMDs in the structure controlled by MTMD against El Centro earthquake. It can be seen that the higher the mass ratio of the first TMD is, the more the displacement of the roof of the structure decreases.

However, if the second TMD gets smaller, its displacement becomes more. Since, in practice, providing a large space for TMD is not possible and reasonable, the mass ratio of the first TMD to the second TMD is considered 80% to 20%.

3.4. Active-Passive Tuned Mass Damper Controller. In the AP-TMD, the actuator is located between the TMDs, and the inactive and active mass dampers are connected to the structure. Due to the location of the actuator between the TMDs, their movement is effective in estimating the control force and should be considered. In this study, four input variables consists of displacement and velocity of the roof, and displacement of two TMDs have been used. The genetic algorithm is used to find suitable rules in order to optimize the structural response. A complete description and configuration of the fuzzy genetic system used are given in Section 7.

Although, in some research, the merits of using fuzzy logic in estimating control force are stated [57], a fuzzy genetic system combines the merits of both passive and active systems by providing active control and reducing power requirements for control force [16, 20, 58].

In MTMD and AP-TMD systems, the mass ratio distribution between the two TMDs is selected in a way that performs best in structural control.

AP-TMD, as shown in Figure 1, consists of two TMDs connected in series, and a stimulus is located between two TMDs. Therefore, the motion of TMDs must be effective in the fuzzy rules of this controller. On the other hand, the control system's purpose is to reduce the structure's response, including displacement, velocity, or acceleration, and these parameters should be considered in the control rules.

Therefore, considering a high number of input variables and membership functions and the impossibility of determining the output of control rules by fuzzy algorithms with the knowledge of an expert, a fuzzy genetic algorithm has been used to control the AP-TMD. In the AP-TMD damper, where the fuzzy control rules are written by a genetic algorithm, the values of α and ζ are optimized by a genetic algorithm.

4. Fuzzy Logic Controller (FLC)

A fuzzy algorithm is used to determine the control force of the ATMD damper. In this controller, the actuator is connected to the structure. The maximum displacement and velocity of the structure on the roof have been used to design a fuzzy algorithm. For the design of the fuzzy system, all the rules in this article are written using the Mamdani method to apply to fuzzification, and the centroid method is used in defuzzification. For each of the input variables of velocity and displacement of the roof in the structure, three triangular membership functions are considered, the example of which is shown in Figure 2. The triangular membership function is extensively used, particularly in real-time applications, because of its simple mathematical formulas and

Table 4: Damping ratio and frequency ratio of MTMD.

	Earthquakes	Frequency ratio of the first TMD	Damping ratio of first TMD	Frequency ratio of the second TMD	Damping ratio of the second TMD
MTMD	El Centro	1.19	0	0.88	0.15
	Hachinohe	0.95	0	0.85	0.15
	Kobe	1.08	0	1.2	0.15
	Northridge	1.12	0	0.8	0.15

Table 5: Comparison of different mass percentages of TMDs in controlled structures with MTMD in El Centro earthquake.

M_{TMD1}/M_{TMD2}	30/70	50/50	70/30	80/20	90/10
Displacement of roof	0.118	0.0985	0.0964	0.0953	0.0932
Displacement of the first TMD	0.1873	0.0987	0.3329	0.2585	0.3112
Displacement of the second TMD	0.2586	0.0989	0.5108	0.6041	1.0112

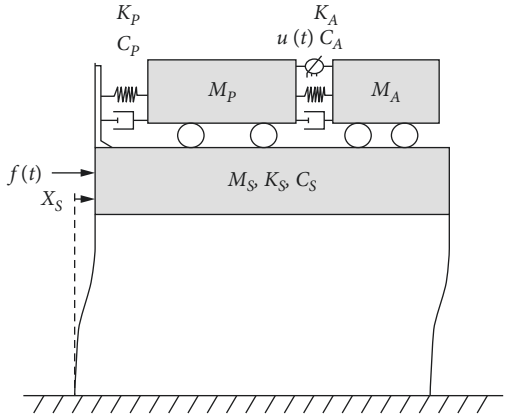

Figure 1: AP-TMD controller.

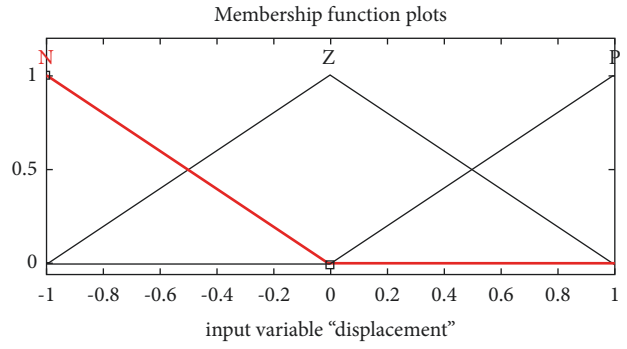

Figure 2: Input membership functions.

efficiency of computation [59]. Three parameters $\{a, b, c\}$ define a triangular membership function [60].

Also, seven triangular membership functions are provided for the control force as the output variable of the fuzzy controller, which are presented in Figure 3.

The concept of input and output variables is written in Table 6.

The fuzzy rule base plays a crucial role in determining the control force and is usually obtained from the knowledge of an expert. Table 7 shows the fuzzy rules database used for ATMD.

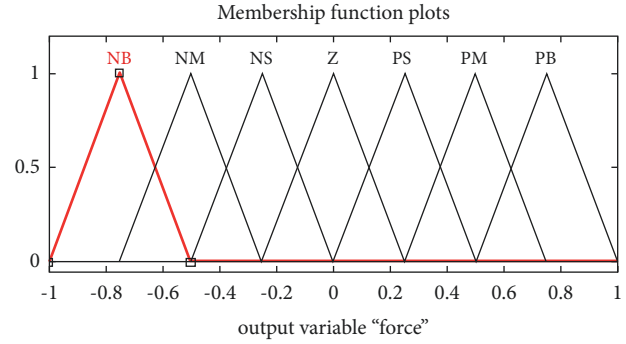

Figure 3: Output membership functions (force).

Table 6: The concept of input and output.

Membership function	Variable	Definition
Input	P	Positive
	Z	Zero
	N	Negative
Output	PB	Positive big
	PM	Positive medium
	PS	Positive small
	Z	Zero
	NS	Negative small
	NM	Negative medium
	NB	Negative big

Table 7: Fuzzy rule database for ATMD.

	Velocity		
Displacement	N	Z	P
N	PB	PM	PS
Z	PS	Z	NS
P	NS	NM	NB

5. The Genetic-Based Fuzzy Logic Controller (GFLC)

In this study, a fuzzy genetic algorithm is used for the creation of the control force and optimization of parameters of AP-TMD.

The basic components common to almost all genetic algorithms are explained as follows:

(i) A fitness function for optimization
(ii) A population of chromosomes
(iii) Selection of which chromosomes will reproduce
(iv) Crossover to produce next generation
(v) Random mutation of chromosomes in a new generation

First, the membership functions of the input and output variables are selected. The displacement of the structure, the displacement of the first TMD, the displacement of the second TMD, and the velocity of the structure are four selected input variables and the control force is the output variable. Each of the input variables has 3 fuzzy values, so the input space is divided into 81 parts, or in other words, the fuzzy rule database contains 81 rules. Determining the outcome of 81 fuzzy rules is a task that the genetic algorithm must perform. MATLAB software and genetic algorithm coding have been used to create a rules database.

In this way, in fuzzy block coding, the output variables are named R1, R2, ... , R81. Each of the R variables can take integers between 1 and 7, in which 1 represents the fuzzy value of NB, 2 represents NM, and with the same respect, 7 represents PB. The genetic algorithm also optimizes the damping and frequency ratio parameters of TMDs (4 parameters) in this controller. Therefore, the number of parameters that the genetic algorithm must determine is 85 totally.

Figures 4 and 5 show the training and optimization process of the fuzzy genetic algorithm as an example for the two earthquakes of El Centro and Kobe. The first graph's horizontal axis shows the population's generation number and the vertical axis shows the value of the objective function. The best response for each generation is shown in the graph, along with the average response obtained for members of each population. In the El Centro earthquake, the best response produced after 80 generations of the initial population is 0.0535, as shown in Figure 4. The second diagram shows the variables optimized by the genetic algorithm, including the fuzzy rules (81 variables), the damping ratio (2 parameters), and the frequency ratio (2 parameters) of two TMDs, with the bar graph in Figure 4.

6. The Optimization of the Genetic Algorithm

The settings of the MATLAB program are effective in the optimization process. Proper selection of GA settings will increase achieving the optimal response and the speed of achieving the desired result. The settings applied to the genetic algorithm used in the research are as follows:

Number of variables: 85
Population type: double vector
Population size: 85
Creation function: feasible population
Selection function: stochastic uniform
Crossover function: scattered
Mutation function: adaptive feasible
Migration: Not used
Crossover rate = 0.8
Mutation rate = 0.2
Termination criteria: maximum number of 100 generations and generation stagnation of 80 generations

6.1. Optimization of Frequency Ratio and Damping Ratio of AP-TMD. In AP-TMD, the parameters α and ζ are optimized with the genetic algorithm, just like the control rules. The genetic algorithm assumes a range of 0.5 to 1.5 times the structural frequency for the frequency ratio and a range of 0 to 0.15 times the structural damping for the damping ratio, like the numerical optimization method of α and ζ for other dampers. Damping and frequency ratios are optimized based on the combination of 70% and 30% of the maximum and RMS of the displacement of the structural roof, respectively. The results of the genetic algorithm in optimizing α and ζ of AP-TMD are given in Table 8. Finally, the frequency and damping ratios of two TMDs are determined and shown in Table 9.

7. Earthquakes

The International Committee related to the Control of Structures has designated four accelerometers to measure the effectiveness of the control methods [61]. These accelerometers include two far-field earthquakes (El Centro and Hachinohe) and two near-field earthquakes (Kobe and Northridge). In the present study, the four accelerometers with scaled intensities are used to determine the effect of dampers. In other words, El Centro and Hachinohe with real intensities, Northridge with 30% real intensity, and Kobe with 40% real intensity are used. Because Kobe and Northridge earthquakes are near-field and high-intensity earthquakes that occur in a short time, large and nonlinear deformations in the structure members are probable. Therefore, in this study, two earthquakes, Kobe and Northridge, have been scaled to keep the structure in the range of elastic deformations.

8. Results

This section compares the performance of different tuned mass dampers in reducing the structure's response. These controllers include tuned mass damper (TMD), active tuned mass damper (ATMD), multituned mass damper (MTMD), and active-passive tuned mass damper (AP-TMD). It should be noted that in order to compare control systems with each other, the percentage of mass is constant and equal to 5% of the total structure' mass.

Stiffness and damping parameters in all controllers are optimized based on the combination of maximum and RMS criteria of roof displacement by 70% and 30%, respectively. Parameters of frequency and damping ratio are optimized

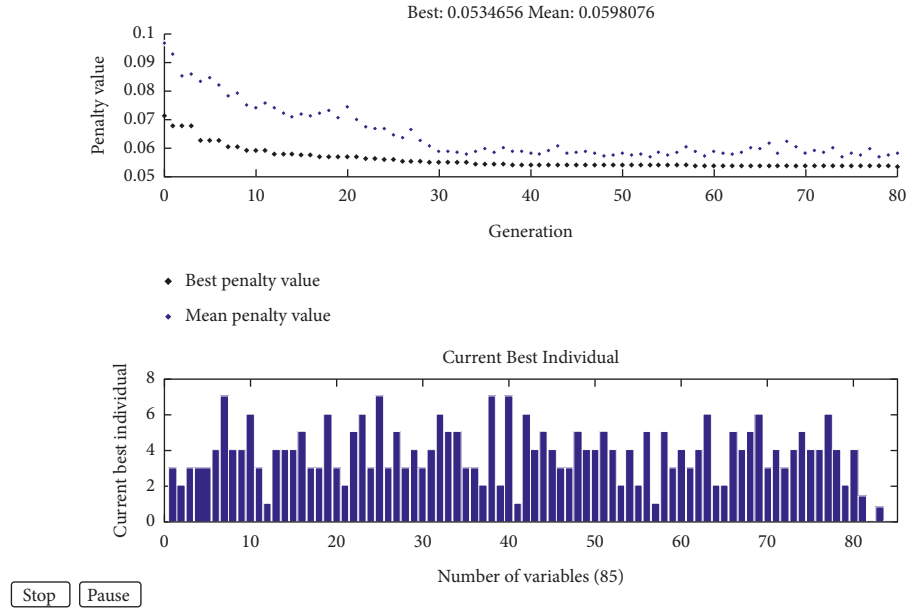

Figure 4: Fuzzy genetic algorithm training process and bar graphs of variables for El Centro earthquake.

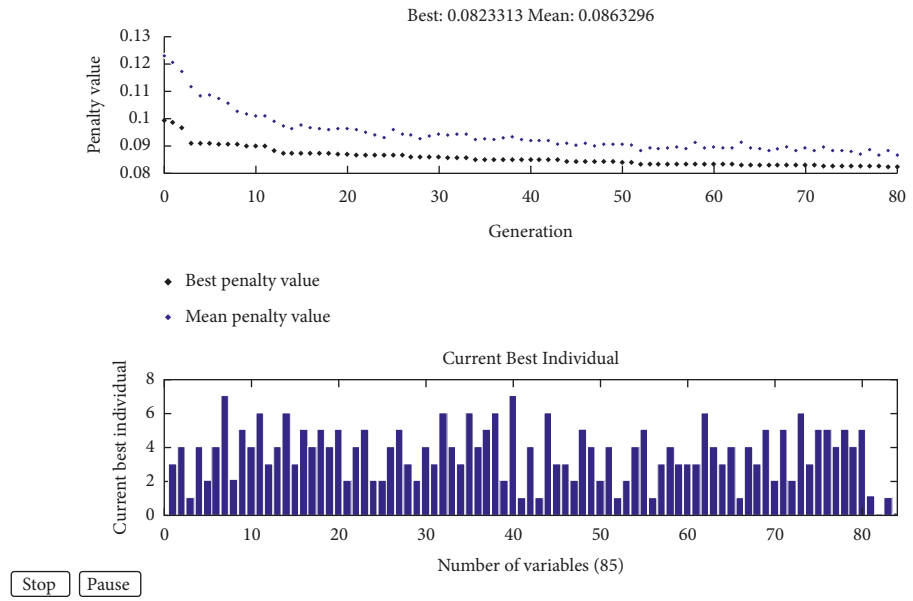

Figure 5: Fuzzy genetic algorithm training process and bar graphs of variables for Kobe earthquake.

Table 8: Upper and lower range of variables.

Range	1–7	0.5–1.5	0–0.15
Variable	1–81	82, 84	83, 85

Table 9: The frequency and damping ratio of AP-TMD with maximum and RMS displacement optimization criteria.

AP-TMD		Frequency ratio of the first TMD	Damping ratio of the first TMD	Frequency ratio of the second TMD	Damping ratio of the second TMD
RMS displacement optimization criteria	El Centro	1.3751	0.0374	0.8278	0.047
	Hachinohe	1.143	0.0239	0.8131	0.122
	Kobe	1.1101	0.0305	1.0093	0.0798
	Northridge	1.2061	0.0567	0.7089	0.0507

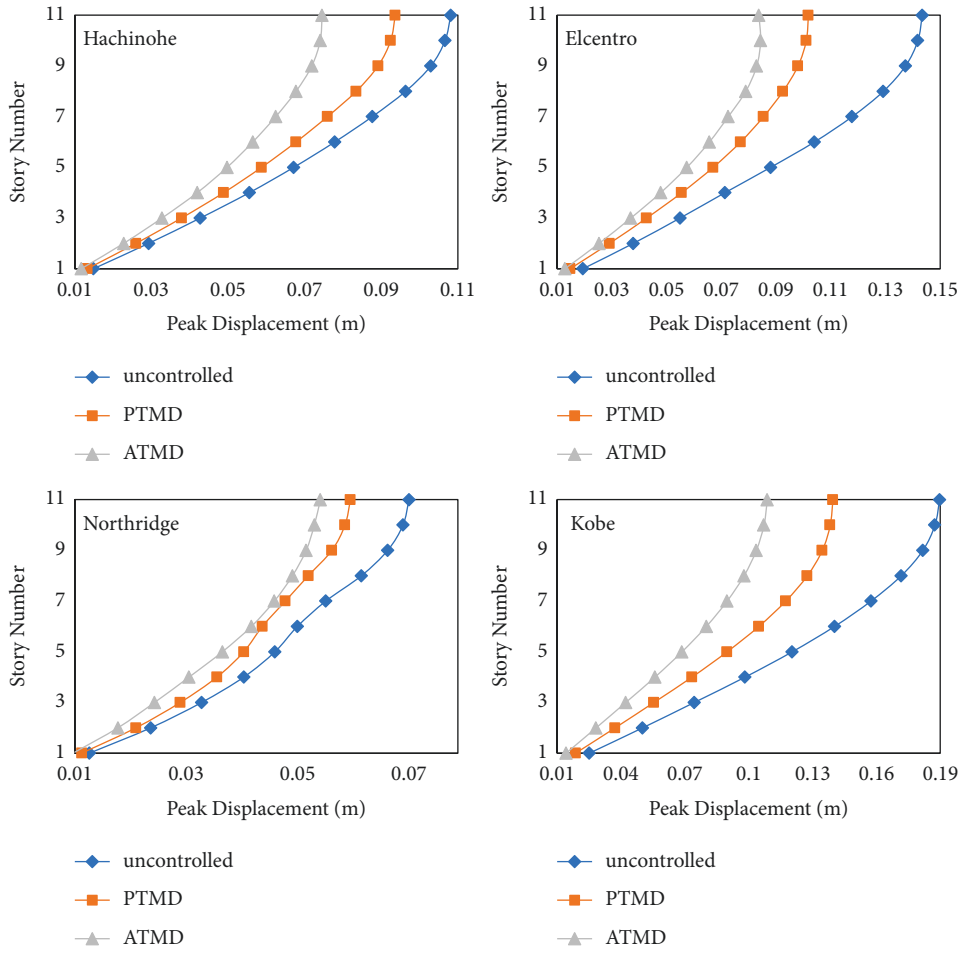

Figure 6: Maximum displacement of structural floors with PTMD and ATMD controller.

based on a numerical method in TMD, MTMD, and ATMD and optimized by a genetic algorithm in AP-TMD. The fuzzy algorithm is used to determine the control force in ATMD. In the AP-TMD system, a genetic algorithm is used to make fuzzy rules due to the effect of TMD motion on the active force between the TMDs and the complexity of its operation. The control rules of this system are set based on the four parameters of roof displacement, roof velocity, and displacement of two TMDs. The programming details of the genetic algorithm in an m-file in MATLAB are provided in Appendix A, and the time history of roof displacement in the AP-TMD system is provided in Appendix B. This section presents the results of maximum and RMS displacement and maximum and RMS acceleration; and finally, the control force is evaluated.

8.1. Results of TMD and ATMD. This part presents the maximum and RMS of displacement in the structure equipped with ATMD under four earthquakes of El Centro, Hachinohe, Kobe, and Northridge. The results are compared with uncontrolled structure and structure with PTMD controller. Although using a controller reduces the displacement of the structure under an earthquake in all cases, the amount of reduction is different due to the acceleration and type of ground motions.

The maximum displacement of structural floors equipped with ATMD is plotted in Figure 6. By using ATMD, the percentage of reduction of maximum response to uncontrolled structure in El Centro, Hachinohe, Kobe, and Northridge earthquakes are 42%, 31%, 43%, and 23%, respectively, and PTMD reduced the response of structures under the El Centro, Hachinohe, Kobe, and Northridge earthquakes by 29%, 13%, 26%, and 15%, respectively. It can be seen that the percentage of response reduction of structures with ATMD in the Northridge earthquake is lower than in others, which is due to the shock nature of this near-field earthquake.

The results of RMS response of structural displacement by ATMD under four selected earthquakes (as shown in Figure 7) are 48%, 52%, 41%, and 9% less than that of uncontrolled structures, respectively. The reduction of RMS response when TMD is employed in structure is 34, 34, 29, and 1% under these earthquakes, respectively.

The performance of structure equipped with ATMD is much better than that with TMD due to applying active control force in the controller. These figures show the effectiveness of using APTD in a structure against various earthquakes.

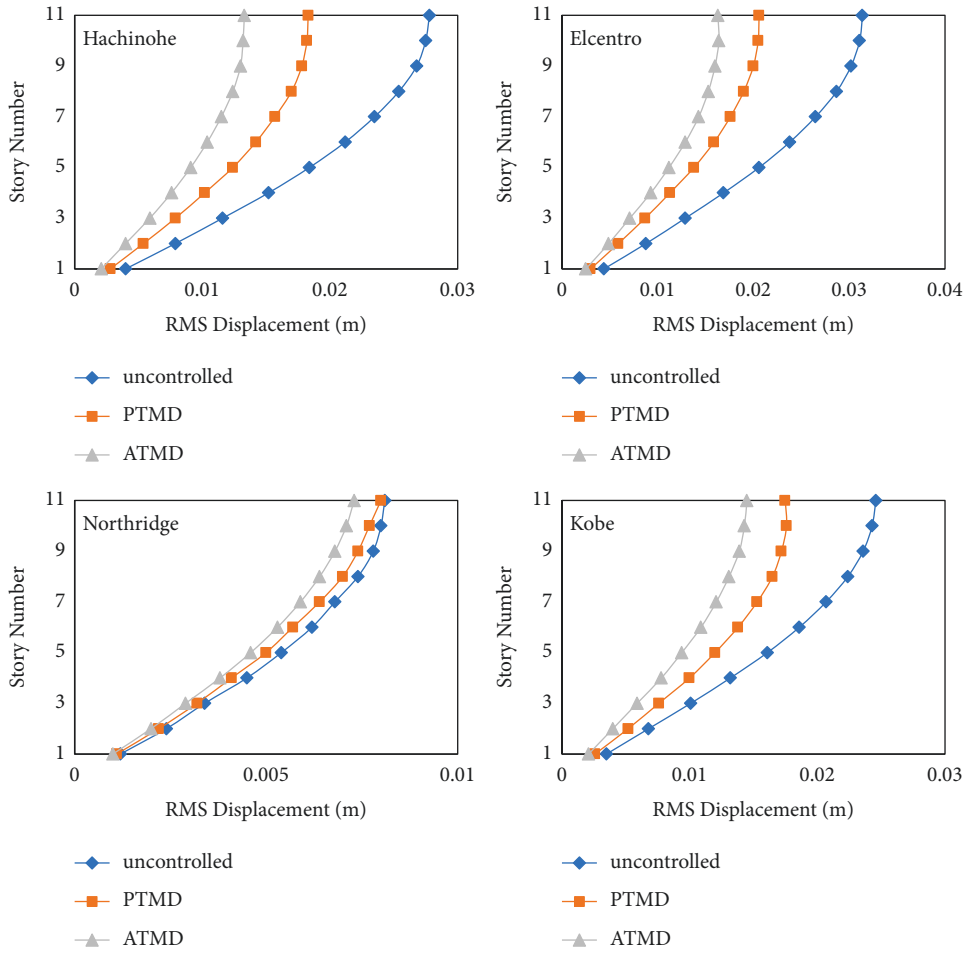

Figure 7: RMS displacement of structural floors with PTMD and ATMD controller.

8.2. Results of MTMD and AP-TMD. In Figures 8 and 9, the maximum displacement of the controlled structure and its RMS are compared with the uncontrolled one under the El Centro, Hachinohe, Kobe, and Northridge earthquakes.

The MTMD controller is also a passive system, consisting of two tuned mass dampers connected in series. The mass ratio (5%) of the damper in this system is divided into 80% and 20% between TMDs, which are connected to the roof of the structure. Based on Figure 8, MTMD reduced the maximum roof displacement by 23% on average. In Figure 9, it can be seen that MTMD has reduced the RMS of displacement by 31 to 38% in the El Centro, Hachinohe, and Kobe earthquakes. However, in the Northridge earthquake, due to the shock nature of the earthquake, the reduction percentage of RMS displacement is 10% and it is much lower than that of other earthquakes. Overall, MTMD reduced RMS displacement by an average of 29% under four earthquakes.

In general, it can be inferred that in a passive system, the maximum displacement and its RMS decreased compared to the uncontrolled structure. Response reduction in each earthquake varies according to the nature of the earthquake acceleration. In far-field earthquakes, the passive controller is effective, but in near-field earthquakes, especially the Northridge earthquake, where the maximum acceleration is like shock and disappears in a short time, the controller does not perform well.

It can be seen that in Figures 8 and 9, the displacement response of the structural roof has been well reduced with the adding the control force. The AP-TMD system is a multiple tuned mass damper in which the actuator is located between the two TMDs. In this system, the main TMD is connected to the structure, and the smaller TMD is actively connected to it. By observing the maximum displacement of the structural floors with the AP-TMD controller in Figure 8, it is clear that this system has had the perfect performance, the reason for which is the use of the fuzzy genetic algorithm for the determination of control force and damper optimization criteria. This algorithm was able to search for suitable fuzzy rules that could satisfy the design criteria. The maximum displacement of the roof of the structure with AP-TMD decreased by 41.7% on average in four earthquakes compared to the uncontrolled structure.

The trend of decreasing the maximum displacement response in different earthquakes shows the intelligent fuzzy genetic algorithm has succeeded in meeting the control criteria by properly making the control rules, resulting in the reduction of the maximum displacement that occurred on

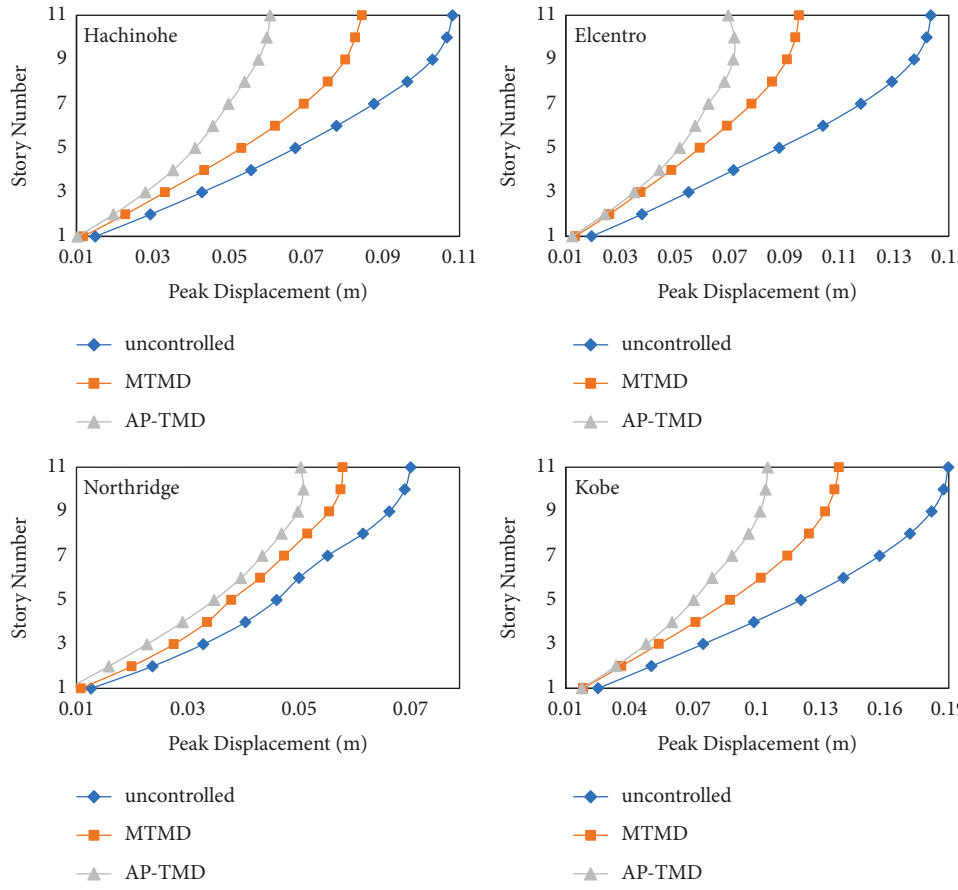

Figure 8: Maximum displacement of structural floors with MTMD and AP-TMD controller.

the roof. Figure 9 shows that the RMS displacements of structure with AP-TMD in the two earthquakes of El Centro and Northridge are well controlled and significantly lower compared with other controllers. Overall, the RMS displacement of the roof of the structure with AP-TMD decreased by an average of 32% compared to the uncontrolled structure.

Figures 10 and 11 demonstrate the reduction of maximum displacement of the structure and its RMS occurred on the roof of the structure. Regarding Figure 10, it can be inferred that AP-TMD could reduce the maximum displacement of structure under four earthquakes 18% more than using MTMD while its performance in RMS displacement is not always better than using MTMD. Therefore, whenever the goal is decreasing the maximum displacement, utilization of AP-TMD is recommended.

8.3. Peak Displacement Results. Figure 12 shows the maximum displacement of the floors in the structure controlled under the El Centro, Hachinohe, Kobe, and Northridge earthquakes. As it can be seen in shapes, AP-TMD performance in reducing the maximum displacements is better than that of other controllers. Also, all controllers reduce the maximum displacements in comparison with uncontrolled structures. Controller PTMD is able to reduce the maximum displacement between 13.5% and 39% in four earthquakes. Using MTMD has approximately similar performance to TMD in all mentioned seismic excitation. Figure 12 shows that the active system performed better in reducing the maximum displacement. The maximum displacement of the structure with ATMD decreased by 42% in the best case among four earthquakes compared to the uncontrolled structure. Moreover, the maximum displacement of structures with AP-TMD in four earthquakes decreased by 41.7% on average compared to uncontrolled structures.

8.4. RMS Acceleration Results. Figure 13 shows the maximum acceleration of the floors in the structure controlled under the El Centro, Hachinohe, Kobe, and Northridge earthquakes. The criterion for optimizing mass dampers is the reduction of the maximum displacement of the structural roof and its RMS simultaneously. Although there is no parameter of structural acceleration in the optimization criterion, diagrams show that in all earthquakes, dampers have been able to control the acceleration response of the structure considerably. Controller PTMD is able to reduce the average roof RMS acceleration up to 22.7% on average in four earthquakes. The reduction percentages of acceleration using PTMD are limited, arising from the limitation of PTMD. MTMD is able to reduce the RMS acceleration better than the PTMD system in all mentioned seismic loads except the Northridge earthquake. The structural roof acceleration

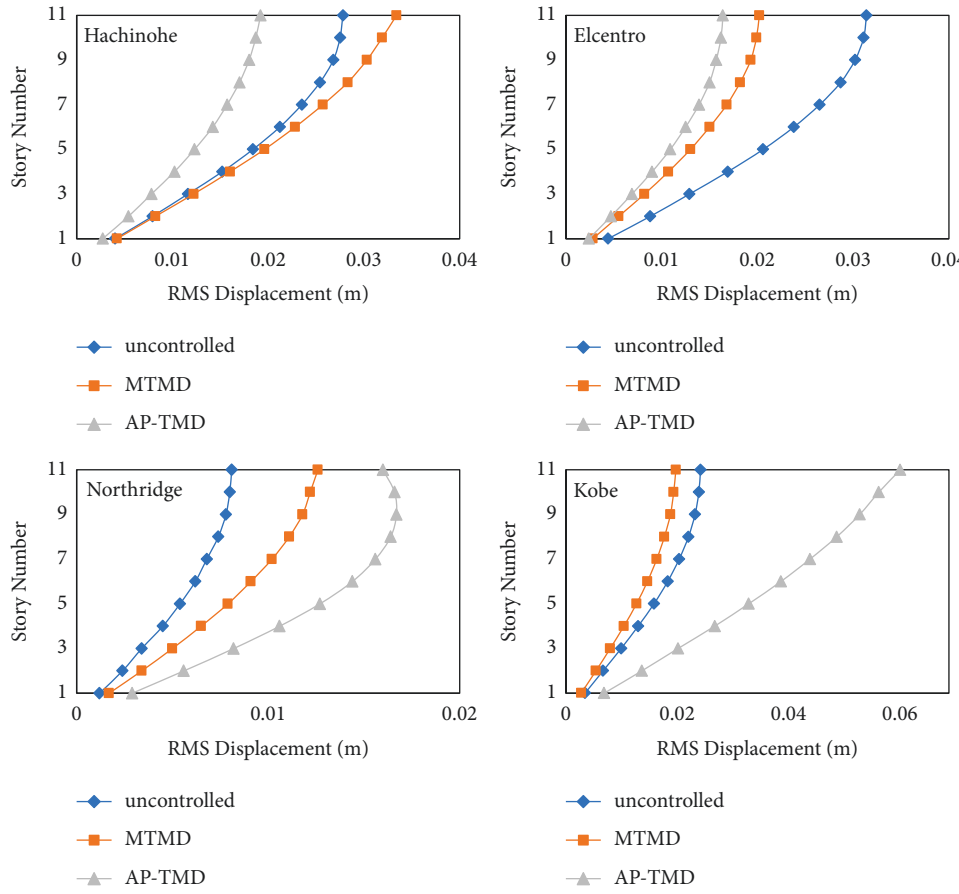

Figure 9: RMS displacement of structural floors with MTMD and AP-TMD controller.

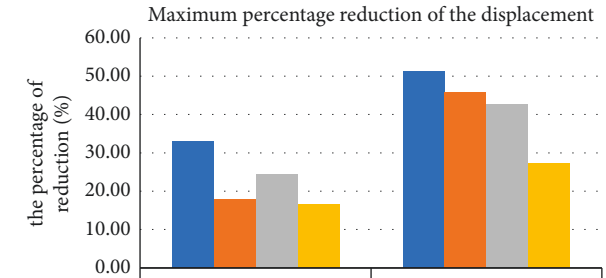

	MTMD	AP-TMD
Elcentro	33.10%	51.15%
Hachinohe	17.93%	45.75%
Kobe	24.42%	42.71%
Northridge	16.60%	27.14%

Figure 10: Maximum percentage reduction of the displacement on the roof of the structure with two controllers.

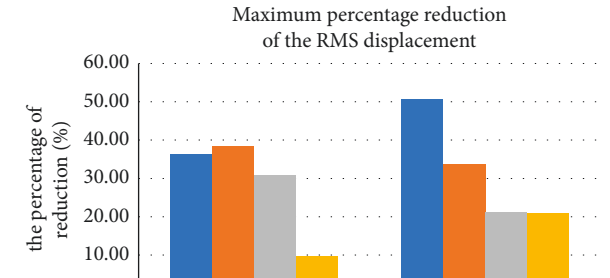

	MTMD	AP-TMD
Elcentro	36.31%	50.64%
Hachinohe	38.49%	33.81%
Kobe	30.89%	21.14%
Northridge	9.88%	20.99%

Figure 11: Maximum percentage reduction of the RMS displacement on the roof of the structure with two controllers.

with MTMD decreased by 26.5% on average in four earthquakes. The RMS diagram of the acceleration of structure equipped with ATMD in all sections of Figure 13 shows that the active system performed better in reducing the RMS acceleration. In all four earthquakes, the acceleration of the RMS has more reduction than that of the other control systems. RMS acceleration of the structure with ATMD decreased by 37.5% on average in four earthquakes compared to the uncontrolled structure. Moreover, the RMS acceleration of structures with AP-TMD in four earthquakes decreased by 27.7% on average compared to uncontrolled structures. Although the genetic algorithm's main focus and optimization criterion has been to reduce the maximum displacement, the reduction of maximum acceleration is also

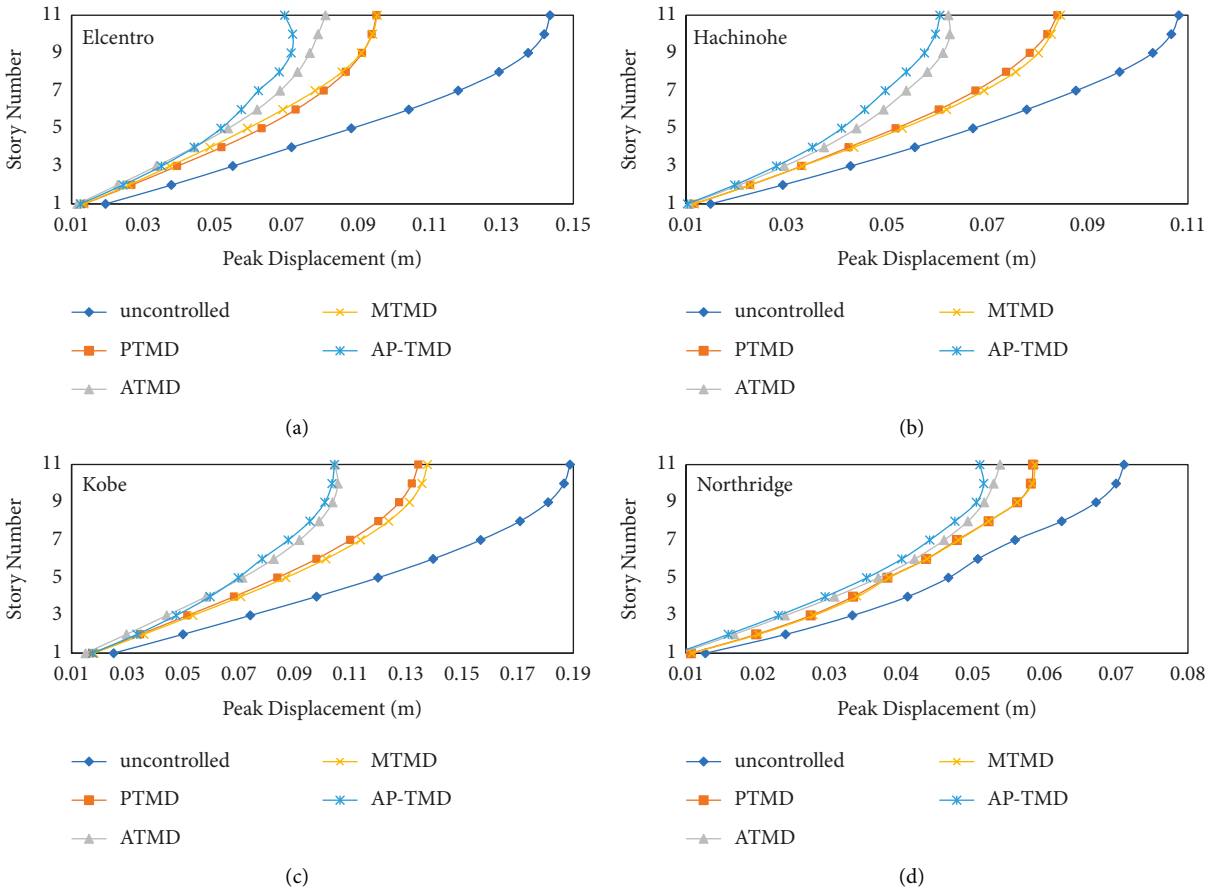

Figure 12: Maximum displacement of structures with different controllers under 4 earthquakes. (a) Maximum displacement of structure under El Centro earthquake. (b) Maximum displacement of structure under Hachinohe earthquake. (c) Maximum displacement of structure under Kobe earthquake. (d) Maximum displacement of structure under Northridge earthquake.

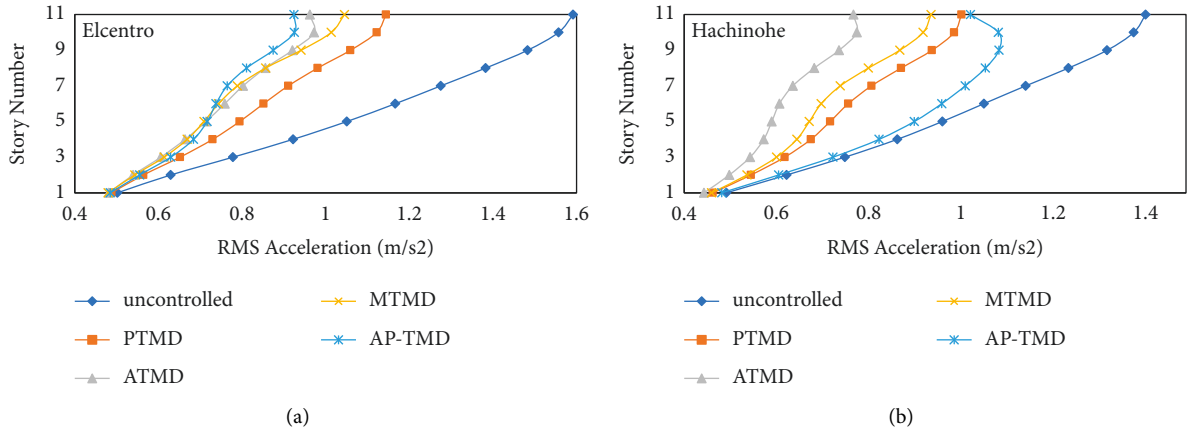

Figure 13: Continued.

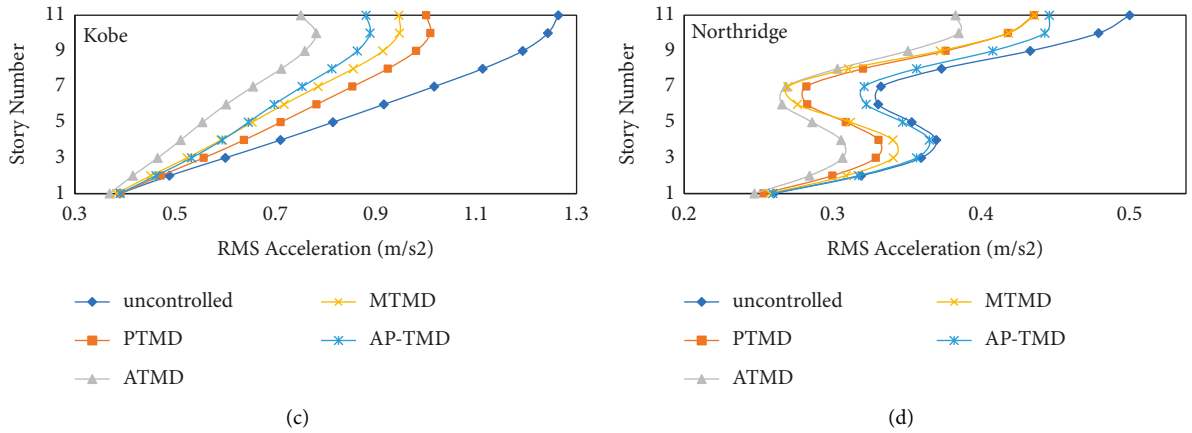

Figure 13: RMS acceleration of structures with different controllers under 4 earthquakes. (a) RMS acceleration of structure under El Centro earthquake. (b) RMS acceleration of structure under Hachinohe earthquake. (c) RMS acceleration of structure under Kobe earthquake. (d) RMS acceleration of structure under Northridge earthquake.

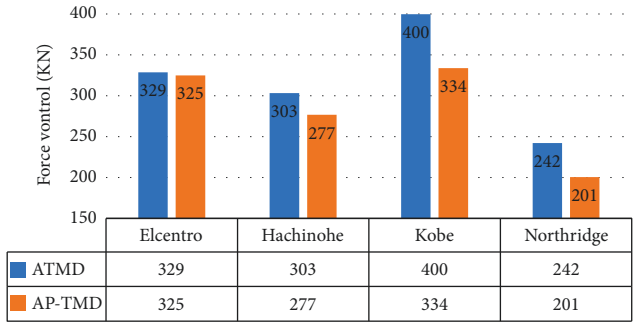

	Elcentro	Hachinohe	Kobe	Northridge
ATMD	329	303	400	242
AP-TMD	325	277	334	201

Figure 14: The control Force of AP-TMD and ATMD.

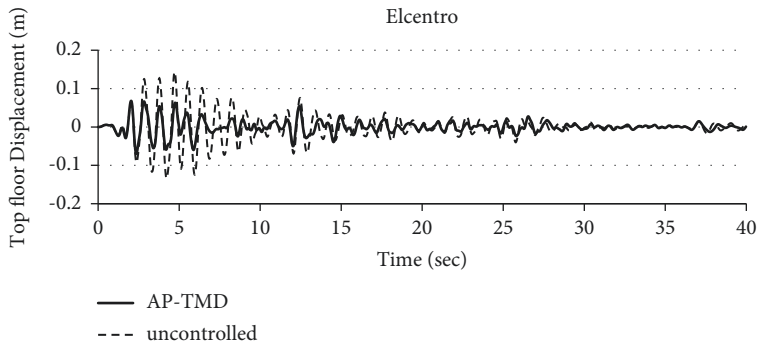

Figure 15: Top floor displacement of structure under Elcentro.

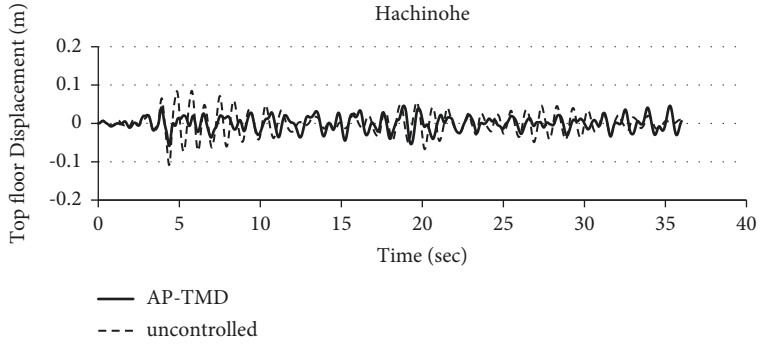

Figure 16: Top floor displacement of structure under Hachinohe.

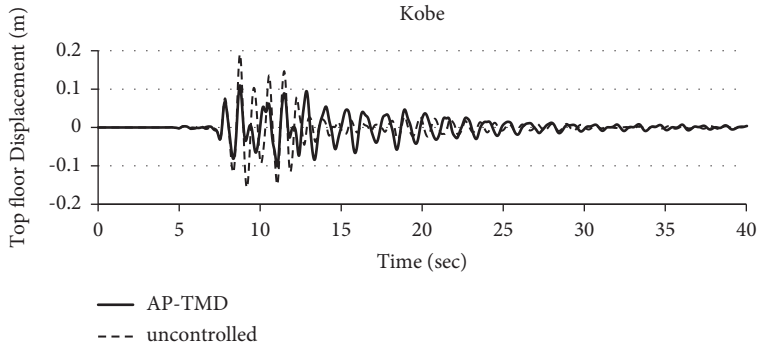

Figure 17: Top floor displacement of structure under Kobe.

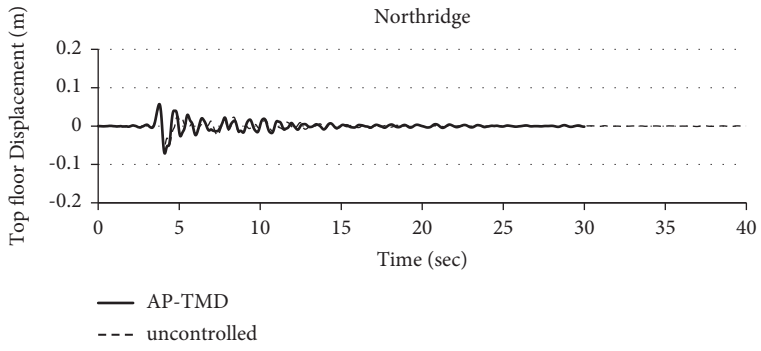

Figure 18: Top floor displacement of structure under Northridge.

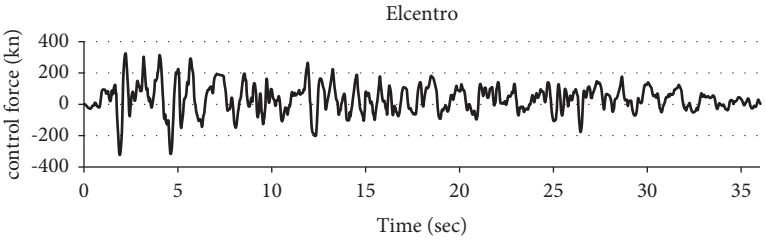

Figure 19: The control force in AP-TMD in Elcentro earthquake.

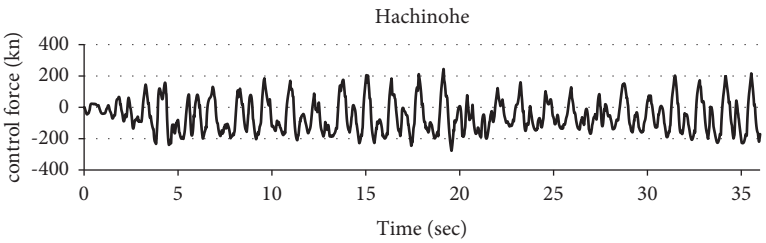

Figure 20: The control force in AP-TMD in Hachinohe earthquake.

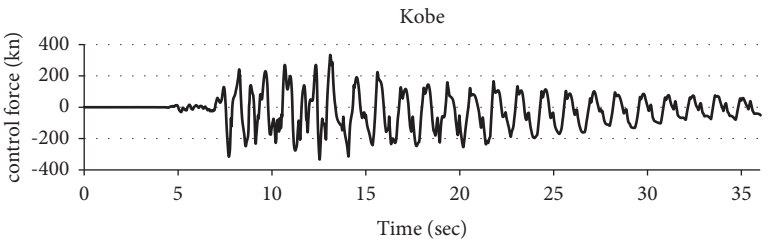

Figure 21: The control force in AP-TMD in Kobe earthquake.

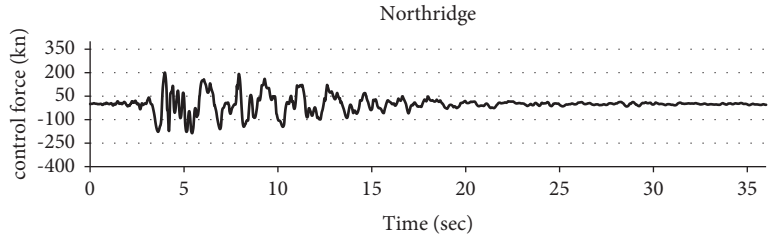

Figure 22: The control force in AP-TMD in Northridge earthquake.

noticeable. Suppose a parameter of structural acceleration was considered in the control criterion. In that case, this scattering does not exist in reducing acceleration, and the AP-TMD system could have performed better in all earthquakes.

9. Results of Control Force

In this section, the control forces of hybrid systems are presented. Figure 14 shows the values of these systems' control force (KN) in four earthquakes. In the AP-TMD system, the genetic algorithm as an intelligent computational algorithm, by considering a set of responses in each computational iteration, effectively searches for fuzzy rules and proceeds to reduce the structure's response considerably. Comparing the control forces in different earthquakes, it can be seen that the control force in the Northridge earthquake is much less than that in other earthquakes and the control force in the Kobe earthquake has the highest value. According to the frequency content of the Northridge and Kobe earthquakes, it can be inferred that although both of them are near-field, the amount of energy shown in the frequency content of the Kobe earthquake is much higher than that in the Northridge earthquake, so it needs more control energy to achieve optimal control. It is noteworthy that the time history of the control force for AP-TMD is presented in Appendix C.

10. Conclusion

The primary purpose of this study was to investigate and compare the performance of PTMD, MTMD, ATMD, and AP-TMD. The control forces employed in ATMD and AP-TMD are calculated sequentially by fuzzy logic and genetic fuzzy logic algorithms. GFLC obtains parameters of TMDs in AP-TMD and in other controllers are examined by numerical analysis. The mass ratios in MTMD and AP-TMD are considered 80% to 20% of the total mass ratio of TMD (5% of structure's mass) and is obtained by numerical analysis.

Some main results are explained as follows:

(1) Using control force in AP-TMD improves the performance of the controller in structural response compared with MTMD.

(2) RMS acceleration of the structure with ATMD decreased by 37.5% on average in four earthquakes compared to the uncontrolled structure and has better effects on RMS acceleration than other controllers' performance.

(3) The maximum displacement of the roof of the structure with AP-TMD decreased by 41.7% on average in four earthquakes compared to the uncontrolled structure.

(4) Control force used to reduce the structural response decreases significantly in AP-TMD compared with ATMD.

(5) The percentage reduction of structural response equipped MTMD or AP-TMD in far-field earthquakes is better than that in near-filed earthquakes; therefore, the controllers perform better in structures under far-field earthquakes.

(6) The ATMD reduced the maximum and RMS displacement of structure by 34% and 37% on average, while TMD has a reduction of 20% and 24% on average, respectively.

(7) Northridge earthquake, as an earthquake with a shock nature reduces the performance of MTMD in reduction of displacement significantly. Such a trend can also be seen when an AP-TMD is used in the structure.

(8) AP-TMD could reduce the maximum displacement of structure under four earthquakes 18% more than using MTMD, while such a better performance does not occur in the reduction of RMS displacement.

(9) AP-TMD has a much better performance in reduction of maximum displacement compared to other controllers.

Appendix

A. Programming for Optimization of Genetic Algorithms

Programs are written for optimization of genetic algorithms, in an m-file format in MATLAB software environment.

```
%%% GA function %%%
function fit = PAfunction(r)
GF = newfis ('GF');
%%%%%%%%%%%%%% input1: displacement of structure %%%%%%%%%%%%%%
GF = addvar (GF, 'input', 'XS', [−1 1]);
GF = addmf (GF, 'input', 1, 'N','trimf', [−2 −1 0]);
GF = addmf (GF, 'input', 1, 'Z', 'trimf', [−1 0 1]);
```

```
GF = addmf (GF, 'input', 1, 'P', 'trimf', [0 1 2]);
%%%%%%%%%%%%% input2: displacement of PTMD %%%%%%%%%%%%%
GF = addvar (GF, 'input', 'XPD', [−1 1]);
GF = addmf (GF, 'input', 2, 'N', 'trimf', [−2 −1 0]);
GF = addmf (GF, 'input', 2, 'Z', 'trimf', [−1 0 1]);
GF = addmf (GF, 'input', 2, 'P', 'trimf', [0 1 2]);
%%%%%%%%%%%%% input3: displacement of ATMD %%%%%%%%%%%%%
GF = addvar (GF, 'input', 'XAD', [−1 1]);
GF = addmf (GF, 'input', 3, 'N', 'trimf', [−2 −1 0]);
GF = addmf (GF, 'input', 3, 'Z', 'trimf',[−1 0 1]);
GF = addmf (GF, 'input', 3, 'P', 'trimf', [0 1 2]);
%%%%%%%%%%%%% input4: velocity of structure %%%%%%%%%%%%
GF = addvar (GF, 'input', 'XdS', [−1 1]);
GF = addmf (GF, 'input', 4, 'N', 'trimf', [−2 −1 0]);
GF = addmf (GF, 'input', 4, 'Z', 'trimf', [−1 0 1]);
GF = addmf (GF, 'input', 4, 'P', 'trimf', [0 1 2]);
%%%%%%%%%%%%% output: control force %%%%%%%%%%%%
GF = addvar (GF, 'output', 'Force', [−1 1]);
GF = addmf (GF, 'output', 1, 'NB', 'trimf', [−1 −0.75−0.5]);
GF = addmf (GF, 'output', 1, 'NM', 'trimf', [−0.75 −0.5 −0.25]);
GF = addmf (GF, 'output', 1, 'NS', 'trimf', [−0.5 −0.25 0]);
GF = addmf (GF, 'output', 1, 'Z', 'trimf', [−0.25 0 0.25]);
GF = addmf (GF, 'output', 1, 'PS', 'trimf', [0 0.25 0.5]);
GF = addmf (GF, 'output', 1, 'PM', 'trimf', [0.25 0.5 0.75]);
GF = addmf (GF, 'output', 1, 'PB', 'trimf', [0.5 0.75 1]);
%%%%%%%%%%%%% rulelist %%%%%%%%%%%%
ruleList = [
1 1 1 1 r (1, 1) 1 1
1 1 1 2 r (1, 2) 1 1
1 1 1 3 r (1, 3) 1 1
1 1 2 1 r (1, 4) 1 1
1 1 2 2 r (1, 5) 1 1
1 1 2 3 r (1, 6) 1 1
1 1 3 1 r (1, 7) 1 1
1 1 3 2 r (1, 8) 1 1
1 1 3 3 r (1, 9) 1 1
1 2 1 1 r (1, 10) 1 1
1 2 1 2 r (1, 11) 1 1
1 2 1 3 r (1, 12) 1 1
1 2 2 1 r (1, 13) 1 1
1 2 2 2 r (1, 14) 1 1
1 2 2 3 r (1, 15) 1 1
1 2 3 1 r (1, 16) 1 1
1 2 3 2 r (1, 17) 1 1
1 2 3 3 r (1, 18) 1 1
1 3 1 1 r (1, 19) 1 1
1 3 1 2 r (1, 20) 1 1
1 3 1 3 r (1, 21) 1 1
1 3 2 1 r (1, 22) 1 1
1 3 2 2 r (1, 23) 1 1
1 3 2 3 r (1, 24) 1 1
1 3 3 1 r (1, 25) 1 1
1 3 3 2 r (1, 26) 1 1
1 3 3 3 r (1, 27) 1 1
2 1 1 1 r (1, 28) 1 1
2 1 1 2 r (1, 29) 1 1
2 1 1 3 r (1, 30) 1 1
2 1 2 1 r (1, 31) 1 1
2 1 2 2 r (1, 32) 1 1
2 1 2 3 r (1, 33) 1 1
2 1 3 1 r (1, 34) 1 1
2 1 3 2 r (1, 35) 1 1
2 1 3 3 r (1, 36) 1 1
2 2 1 1 r (1, 37) 1 1
2 2 1 2 r (1, 38) 1 1
2 2 1 3 r (1, 39) 1 1
2 2 2 1 r (1, 40) 1 1
2 2 2 2 r (1, 41) 1 1
2 2 2 3 r (1, 42) 1 1
2 2 3 1 r (1, 43) 1 1
2 2 3 2 r (1, 44) 1 1
2 2 3 3 r (1, 45) 1 1
2 3 1 1 r (1, 46) 1 1
2 3 1 2 r (1, 47) 1 1
2 3 1 3 r (1, 48) 1 1
2 3 2 1 r (1, 49) 1 1
2 3 2 2 r (1, 50) 1 1
2 3 2 3 r (1, 51) 1 1
2 3 3 1 r (1, 52) 1 1
2 3 3 2 r (1, 53) 1 1
2 3 3 3 r (1, 54) 1 1
3 1 1 1 r (1, 55) 1 1
3 1 1 2 r (1, 56) 1 1
3 1 1 3 r (1, 57) 1 1
3 1 2 1 r (1, 58) 1 1
3 1 2 2 r (1, 59) 1 1
3 1 2 3 r (1, 60) 1 1
3 1 3 1 r (1, 61) 1 1
3 1 3 2 r (1, 62) 1 1
3 1 3 3 r (1, 63) 1 1
```

```
3 2 1 1 r (1, 64) 1 1
3 2 1 2 r (1, 65) 1 1
3 2 1 3 r (1, 66) 1 1
3 2 2 1 r (1, 67) 1 1
3 2 2 2 r (1, 68) 1 1
3 2 2 3 r (1, 69) 1 1
3 2 3 1 r (1, 70) 1 1
3 2 3 2 r (1, 71) 1 1
3 2 3 3 r (1, 72) 1 1
3 3 1 1 r (1, 73) 1 1
3 3 1 2 r (1, 74) 1 1
3 3 1 3 r (1, 75) 1 1
3 3 2 1 r (1, 76) 1 1
3 3 2 2 r (1, 77) 1 1
3 3 2 3 r (1, 78) 1 1
3 3 3 1 r (1, 79) 1 1
3 3 3 2 r (1, 80) 1 1
3 3 3 3 r (1, 81) 1 1];
GF = addrule (GF, ruleList);
writefis (GF, 'GF');
%%%%%%%%%%%%%%%%%%%%%%%%%%%%%%%%%%%%%%%%%%%%%%%%%%%%%%%%%%%%%%%%%%%%%%%%%%%%
%%% GA Run %%%
%%%%%%%%%%%%%%%%%%%%%%%%%%%%%%%%%%%%%%%%%%%%%%%%%%%%%%%%%%%%%%%%%%%%%%%%%%%%
Clc
%%%%%%%%%%%%% Bounds %%%%%%%%%%%%
LB (1 : 1:81) = 1; LB (82) = 0.5; LB (83) = 0; LB (84) = 0.5; LB (85) = 0;
UB (1 : 1:81) = 7; UB (82) = 1.5; UB (83) = 0.15; UB (84) = 1.5; UB (85) = 0.15;
IntCon = 1 : 81;
%%%%%%%%%%%%% GA options set %%%%%%%%%%%%
options = gaoptimset;
options = gaoptimset (options, 'populationtype', 'doublevector');
options = gaoptimset (options, 'stallGenLimit', 80);
options = gaoptimset (options, 'generations', 100);
options = gaoptimset (options, 'populationsize', 85);
options = gaoptimset (options, 'creationFcn', @gacreationlinearfeasible);
options = gaoptimset (options, 'CrossoverFcn', @crossoverscattered);
options = gaoptimset (options, 'MutationFcn', @mutationadaptfeasible);
options = gaoptimset (options, 'outputfcns', {[]});
options = gaoptimset (options, 'Elitecount', 2);
options = gaoptimset (options, 'Display', 'final');
options = gaoptimset (options, 'plotfcns', {@gaplotbestf,@gaplotbestindiv});
options = gaoptimset (options, 'CrossoverFraction', 0.8);
%%%%%%%%%%%% Run %%%%%%%%%%%%
[r, na] = ga (@PAfunction, 85, [], [], [], [], LB, UB, [], IntCon, options);
```

B. Time History of Displacement

Time history of top floor displacement of structure equipped with AP-TMD under four mentioned earthquakes are shown in Appendix B. (Figures15–18)

C. Time History of Control Force

Time history of control force of AP-TMD under four earthquakes are illustrated in Appendix C. (Figures 19–22)

Data Availability

We used data of a paper (Pourzeynali, S., H. H. Lavasani, and A. H. Modarayi. "Active control of high-rise building structures using fuzzy logic and genetic algorithms." Engineering Structures 29.3 (2007): 346-357).

Conflicts of Interest

The authors declare that they have no conflicts of interest.

References

[1] B. F. Spencer Jr and S. Nagarajaiah, "State of the art of structural control," *Journal of Structural Engineering*, vol. 129, no. 7, pp. 845–856, 2003.

[2] N. R. Fisco and H. Adeli, "Smart structures: Part I-Active and semi-active control," *Scientia Iranica*, vol. 18, no. 3, pp. 275–284, 2011.

[3] N. R. Fisco and H. Adeli, "Smart structures: Part II - Hybrid control systems and control strategies," *Scientia Iranica*, vol. 18, no. 3, pp. 285–295, 2011.

[4] G. E. Thermou, S. J. Pantazopoulou, and A. S. Elnashai, "Design methodology for seismic upgrading of substandard reinforced concrete structures," *Journal of Earthquake Engineering*, vol. 11, no. 4, pp. 582–606, 2007.

[5] S. Elias and V. Matsagar, "Research developments in vibration control of structures using passive tuned mass dampers," *Annual Reviews in Control*, vol. 44, pp. 129–156, 2017.

[6] M.-H. Shih and W.-P. Sung, "Seismic resistance and parametric study of building under control of impulsive semi-active mass damper," *Applied Sciences*, vol. 11, no. 6, p. 2468, 2021.

[7] Z. Lu, D. Wang, and Y. Zhou, "Experimental parametric study on wind-induced vibration control of particle tuned mass damper on a benchmark high-rise building," *The Structural Design of Tall and Special Buildings*, vol. 26, no. 8, p. e1359, 2017.

[8] B. Zhao, H. Wang, Z. Lu, and Z. Lu, "Shaking table test on vibration control effects of a monopile offshore wind turbine with a tuned mass damper," *Wind Energy*, vol. 21, no. 12, pp. 1309–1328, 2018.

[9] Z. Lu, D. Chen, K. Zhang, and K. Dai, "Experimental and analytical study on the performance of particle tuned mass dampers under seismic excitation," *Earthquake Engineering & Structural Dynamics*, vol. 46, no. 5, pp. 697–714, 2017.

[10] Z. Lu, X. Chen, and Y. Zhou, "An equivalent method for optimization of particle tuned mass damper based on experimental parametric study," *Journal of Sound and Vibration*, vol. 419, pp. 571–584, 2018.

[11] Z. Lu, W. Lu, S. F. Lu, and S. F. Masri, "Shaking table test of the effects of multi-unit particle dampers attached to an MDOF system under earthquake excitation," *Earthquake Engineering & Structural Dynamics*, vol. 41, no. 5, pp. 987–1000, 2012.

[12] Z. Lu, Q. Huang, X. Zhang, and X. Lu, "Experimental and analytical study on vibration control effects of eddy-current tuned mass dampers under seismic excitations," *Journal of Sound and Vibration*, vol. 421, pp. 153–165, 2018.

[13] H. Gao, C. Wang, W. Huang, L. Shi, and L. Huo, "Development of a frequency-adjustable tuned mass damper (FATMD) for structural vibration control," *Shock and Vibration*, vol. 2020, pp. 1–16, 2020.

[14] M. Yamamoto and T. Sone, "Behavior of active mass damper (AMD) installed in high-rise building during 2011 earthquake off Pacific coast of Tohoku and verification of regenerating system of AMD based on monitoring," *Structural Control and Health Monitoring*, vol. 21, no. 4, pp. 634–647, 2014.

[15] R. Alkhatib and M. F. Golnaraghi, "Active structural vibration control: a review," *The Shock and Vibration Digest*, vol. 35, no. 5, pp. 367–383, 2003.

[16] C.-C. Lin, G.-L. Lin, and J.-Fu Wang, "Protection of seismic structures using semi-active friction TMD," *Earthquake Engineering & Structural Dynamics*, vol. 39, no. 6, pp. 635–659, 2010.

[17] G.-L. Lin, L. Y. Lin, Y. B. Lu, and Y.-B. Ho, "Experimental verification of seismic vibration control using a semi-active friction tuned mass damper," *Earthquake Engineering & Structural Dynamics*, vol. 41, no. 4, pp. 813–830, 2012.

[18] S. Nagarajaiah and E. Sonmez, "Structures with semiactive variable stiffness single/multiple tuned mass dampers," *Journal of Structural Engineering*, vol. 133, no. 1, pp. 67–77, 2007.

[19] S. Nagarajaiah, "Adaptive passive, semiactive, smart tuned mass dampers: identification and control using empirical mode decomposition, hilbert transform, and short-term fourier transform," *Structural Control and Health Monitoring*, vol. 16, no. 7-8, pp. 800–841, 2009.

[20] M.-Ho Chey, J. G. Chase, J. B. Mander, and A. J. Carr, "Semi-active tuned mass damper building systems: design," *Earthquake Engineering & Structural Dynamics*, vol. 39, no. 2, pp. 119–139, 2010.

[21] M.-Ho Chey, J. G. Chase, J. B. Mander, and A. J. Carr, "Semi-active tuned mass damper building systems: Application," *Earthquake Engineering & Structural Dynamics*, vol. 39, no. 1, pp. 69–89, 2010.

[22] R. Soto-Brito and S. E. Ruiz, "Influence of ground motion intensity on the effectiveness of tuned mass dampers," *Earthquake Engineering & Structural Dynamics*, vol. 28, no. 11, pp. 1255–1271, 1999.

[23] P. Lukkunaprasit and A. Wanitkorkul, "Inelastic buildings with tuned mass dampers under moderate ground motions from distant earthquakes," *Earthquake Engineering & Structural Dynamics*, vol. 30, no. 4, pp. 537–551, 2001.

[24] G. Chen and J. Wu, "Experimental study on multiple tuned mass dampers to reduce seismic responses of a three-storey building structure," *Earthquake Engineering & Structural Dynamics*, vol. 32, no. 5, pp. 793–810, 2003.

[25] T. Pinkaew, P. Lukkunaprasit, and P. J. E. S. Chatupote, "Seismic effectiveness of tuned mass dampers for damage reduction of structures," *Engineering Structures*, vol. 25, no. 1, pp. 39–46, 2003.

[26] K. Xu and T. Igusa, "Dynamic characteristics of multiple substructures with closely spaced frequencies," *Earthquake Engineering & Structural Dynamics*, vol. 21, no. 12, pp. 1059–1070, 1992.

[27] U. Aldemir, "Optimal control of structures with semiactive-tuned mass dampers," *Journal of Sound and Vibration*, vol. 266, no. 4, pp. 847–874, 2003.

[28] F. Ricciardelli, A. Occhiuzzi, and P. Clemente, "Semi-active tuned mass damper control strategy for wind-excited structures," *Journal of Wind Engineering and Industrial Aerodynamics*, vol. 88, no. 1, pp. 57–74, 2000.

[29] C. C. Chang and H. T. Y. Yang, "Control of buildings using active tuned mass dampers," *Journal of Engineering Mechanics*, vol. 121, no. 3, pp. 355–366, 1995.

[30] C. Li, Y. Liu, and Z. Wang, "Active multiple tuned mass dampers: a new control strategy," *Journal of Structural Engineering*, vol. 129, no. 7, pp. 972–977, 2003.

[31] M. Jamil, S. J. Khan, Q. Rind, M. Awais, and M. Uzair, "Neural network predictive control of vibrations in tall structure: an experimental controlled vision," *Computers & Electrical Engineering*, vol. 89, no. 2021, p. 106940, Article ID 106940, 2021.

[32] M. Zabihi-Samani and M. Ghanooni-Bagha, "Optimal semi-active structural control with a wavelet-based cuckoo-search fuzzy logic controller," *Iranian Journal of Science and Technology, Transactions of Civil Engineering*, vol. 43, no. 4, pp. 619–634, 2019.

[33] S. Aizawa, "An experimental study on the active mass damper," *Proceedings of Ninth World Conference on Earthquake Engineering*, vol. 5, 1988.

[34] F. Y. Cheng, *Smart Structures: Innovative Systems for Seismic Response Control*, CRC Press, 2008.

[35] T. T. Soong and B. F. Spencer Jr., "Supplemental energy dissipation: state-of-the-art and state-of-the-practice," *Engineering Structures*, vol. 24, no. 3, pp. 243–259, 2002.

[36] M. Sakamoto, "Practical applications of active and hybrid response control systems and their verifications by earthquake and strong wind observations," *Proc. 1st World Conf. on Struct. Control*, 1994.

[37] M. Yamamoto, "Control effects of active mass damper system installed on actual buildings," *Proceedings of the First World Conference on Structural Control*, vol. 3, 1994.

[38] C. M. Wang, N. Yan, and T. Balendra, "Control on dynamic structural response using active-passive composite-tuned mass dampers," *Journal of Vibration and Control*, vol. 5, no. 3, pp. 475–489, 1999.

[39] I. Nishimura, T. Kobori, M. Sakamoto et al., "Active passive composite tuned mass damper," in *Proceedings of the Seminar on Seismic Isolation, Passive Energy Dissipation and Active Control*, pp. 737–748, San Francisco, 1993.

[40] I. Nishimura, M. Sakamoto, T. Yamada, N. Koshika, and T. Kobori, "Acceleration feedback method applied to active-passive composite tuned mass damper," *Journal of Structural Control*, vol. 1, no. 1-2, pp. 103–116, 1994.

[41] I. Fukushima, K. Sasaki, I. Nishimura, N. Koshika, M. Sakamoto, and T. Kobori, "Development and application of active– passive composite tuned mass damper to high-rise building," *Proceedings of Pacic Conference on Earthquake Engineering*, pp. 267–276, 1995.

[42] C. Li, "Multiple active-passive tuned mass dampers for structures under the ground acceleration," *Earthquake Engineering & Structural Dynamics*, vol. 32, no. 6, pp. 949–964, 2003.

[43] K.-M. Choi, H. J. Cho, I. W. Jung, and I.-W. Lee, "Semi-active fuzzy control for seismic response reduction using magnetorheological dampers," *Earthquake Engineering & Structural Dynamics*, vol. 33, no. 6, pp. 723–736, 2004.

[44] M. K. Bhardwaj and T. K. Datta, "Semiactive fuzzy control of the seismic response of building frames," *Journal of Structural Engineering*, vol. 132, no. 5, pp. 791–799, 2006.

[45] H.-Su Kim and P. N. Roschke, "Design of fuzzy logic controller for smart base isolation system using genetic algorithm," *Engineering Structures*, vol. 28, no. 1, pp. 84–96, 2006.

[46] S. Pourzeynali, H. H. Lavasani, and A. H. Modarayi, "Active control of high rise building structures using fuzzy logic and genetic algorithms," *Engineering Structures*, vol. 29, no. 3, pp. 346–357, 2007.

[47] B. Samali, K. C. S. Al-Dawod, F. Kwok, and F. Naghdy, "Active control of cross wind response of 76-story tall building using a fuzzy controller," *Journal of Engineering Mechanics*, vol. 130, no. 4, pp. 492–498, 2004.

[48] M. Al-Dawod, B. Samali, F. Kwok, and F. Naghdy, "Fuzzy controller for seismically excited nonlinear buildings," *Journal of Engineering Mechanics*, vol. 130, no. 4, pp. 407–415, 2004.

[49] H.-Su Kim and P. N. Roschke, "GA-fuzzy control of smart base isolated benchmark building using supervisory control technique," *Advances in Engineering Software*, vol. 38, no. 7, pp. 453–465, 2007.

[50] L. A. Zadeh, "Fuzzy sets," in *Advances in Fuzzy Systems - Applications and Theory*pp. 394–432, Binghamton, USA, 1996.

[51] H. M. Gomes, "Fuzzy logic for structural system control," *Latin American Journal of Solids and Structures*, vol. 9, no. 1, pp. 111–129, 2012.

[52] A. I. Al-Odienat, A. A. Al-Lawama, and A. A. Al-Lawama, "The advantages of PID fuzzy controllers over the conventional types," *American Journal of Applied Sciences*, vol. 5, no. 6, pp. 653–658, 2008.

[53] T.-L. Teng, C.-P. Peng, and C. Chuang, "A study on the application of fuzzy theory to structural active control," *Computer Methods in Applied Mechanics and Engineering*, vol. 189, no. 2, pp. 439–448, 2000.

[54] J. H. Holland, "Adaptation in natural and Artificial systems," in *Applying Genetic Algorithm to Increase the Efficiency of a Data Flow-Based Test Data Generation Approach*, pp. 1–5, The University of Michigan Press, Ann Arbor, MI, 1975.

[55] D. E. Goldberg and J. H. Holland, "Genetic algorithms and machine learning," *Machine Learning*, vol. 3, no. 2/3, pp. 95–99, 1988.

[56] Y.-J. Cha, L. Raich, A. Barroso, and A. Agrawal, "Optimal placement of active control devices and sensors in frame structures using multi-objective genetic algorithms," *Structural Control and Health Monitoring*, vol. 20, no. 1, pp. 16–44, 2013.

[57] F. Hadizadeh, H. Shariatmadar, and F. Akhlaghi Amiri, "The effects of MTMD and HBI on the performance of a benchmark building against near-field earthquakes using fuzzy logic," *Iranian Journal of Science and Technology, Transactions of Civil Engineering*, pp. 1–14, 2022.

[58] S. Nagarajaiah and N. Varadarajan, "Short time Fourier transform algorithm for wind response control of buildings with variable stiffness TMD," *Engineering Structures*, vol. 27, no. 3, pp. 431–441, 2005.

[59] G. Castellano and A. M. Fanelli, "Design of Transparent Mamdani fuzzy," *Design and application of hybrid intelligent systems*, vol. 104, p. 468, 2003.

[60] M. H. Azam, H. H. Mohd, H. Saima, and J. A. Said, "Fuzzy type-1 triangular membership function approximation using fuzzy C-means," in *Proceedings of the 2020 International Conference on Computational Intelligence (ICCI)*, IEEE, Bandar Seri Iskandar, Malaysia, October 2020.

[61] B. Samali and M. Al-Dawod, "Performance of a five-storey benchmark model using an active tuned mass damper and a fuzzy controller," *Engineering Structures*, vol. 25, no. 13, pp. 1597–1610, 2003.